Dipartimento di Ingegneria
Idraulica e Ambientale
Università di Pavia

A Smoothed Particle Hydrodynamics: Basics and Applications

Dr. Sauro Manenti
Giovedì 12 Novembre, 2009
Dipartimento di Meccanica Strutturale - Università degli Studi di Pavia

Abstract

Starting from meshfree methods, the Smoothed Particle Hydrodynamics (SPH) is introduced as a complementary tool for numerical simulation of peculiar hydrodynamic problems: its potential advantages with respect to traditional grid-based techniques are pointed out.

The governing fluid dynamic equations are recalled and their numerical discretization in the SPH approximation is illustrated. Further numerical aspects relevant to SPH are also discussed, such as solid boundaries treatment.

Finally some applications of the SPH method for simulating engineering hydraulic problems are shown, involving rapidly varied free surface flows with large displacements and impacts, scouring phenomena and interaction with rigid bodies.

Purposes and Outline of the Work

This work aims at provide the basic knowledge on the Smoothed Particle Hydrodynamics method (SPH) for numerical application to hydrodynamic problems including interaction with rigid solid body.

The structure of the work consists of the following sections:

1. Grid-based and meshless methods.
2. Basics of the SPH method with mathematical and numerical fundamentals.
3. Implementation of the SPH method on the Navier-Stokes Eq.s.
4. Application of the SPH method to free-surface hydrodynamic problem including interaction with solid rigid body.

1. Grid-Based and Meshless Methods

1.1 The Role of Numerical Modeling

Numerical simulation translates important aspects of the physical problem into a discrete form of mathematical description.

Numerical simulation has become a very important tools in the analysis of complex engineering problems owing to the increasing computers capabilities, their versatility of application and the removal of the numerous assumptions for the achievement of an analytical solution.

However numerical simulation is strongly interconnected to physical and theoretical models owing to some intrinsic lacks (e.g. needs of calibration and validation through experimental data and exact solutions) that limits their reliability as an individual instrument of investigation.

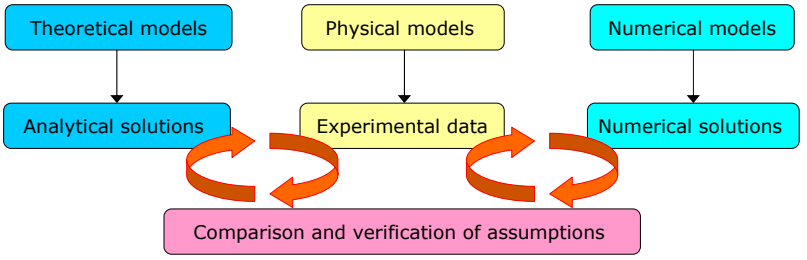

1.1 Numerical Solution Strategy

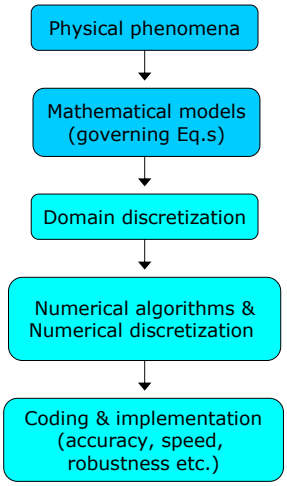

[Liu & Liu, 2007]

The general flow-chart followed by several numerical simulation techniques is shown at the left-hand side.

Starting from the physical phenomenon and focusing on those aspects relevant to the investigation, a simplified mathematical model is derived in the form of governing Eq.s and limit conditions (Initial and/or Boundary Eq.s).

The first step to numerically solve the above set of Eq.s consists of domain discretization (i.e. the continuum is represented by discrete components or elements connected through nodes).

It is followed by numerical discretization to obtain discrete representation of the governing Eq.s according to domain discretization technique.

A set of ordinary differential Eq.s with respect to time is obtained for transient problems: these should be translate into a computer code.

1.2 Grid-Based Methods

Grid-based methods adopt a computational frame which is made up of nodes, where the field variables are evaluated, that are related each other through a predefined nodal connectivity: accuracy of numerical approximation is closely related to mesh topography (shape, size etc.).

There are two fundamental approach for domain discretization:

Lagrangian approach: follows a material description.

The computational grid is assumed to be attached to the continuum following its deformation: no mass flux occurs between adjacent elements.

E.g. Finite Element Method [**Zienkiewicz & Taylor, 1989**]

Finite element model of an off-shore wind turbine [**Bontempi et al. 2006a**].

1.2 Grid-Based Methods

Grid-based methods adopt a computational frame which is made up of nodes, where the field variables are evaluated, that are related each other through a predefined nodal connectivity: accuracy of numerical approximation is closely related to mesh topography (shape, size etc.).

There are two fundamental approach for domain discretization:

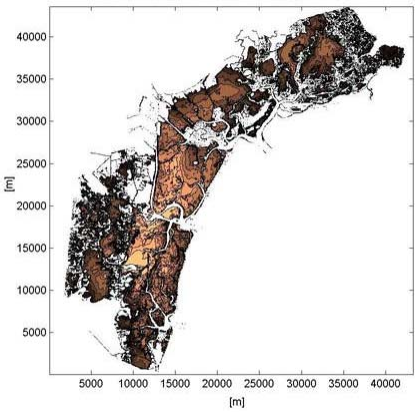

Eulerian approach: follows a spatial description.

The computational grid is assumed to be fixed on the physical space: no deformation occurs as the continuum evolves; mass flux between adjacent cells have to be simulated.

E.g. Finite Difference Method

Finite difference model of the Venice lagoon for wind-wave analysis [**Manenti et al. 2006b**].

1.2 Comparison of Grid-Based Methods

The complementary pros and cons of each method are summarized below:

Lagrangian approach

+ the lack of convective term in the governing equation simplified their numerical handling;

+ it becomes easy to track the time-history of the field variables at a material point;

+ the mesh can adapt to irregular and complex geometries and describes free or moving boundaries and material interfaces;

+ no grid point is needed outside the continuum;

- large deformation of the continuum and following high mesh distortion can negatively affect the numerical accuracy;

- the adaptive mesh rezoning technique can overcome the above problem but introduces much computational effort.

Eulerian approach

- convective transport should be simulated and can influence the integration time step;

- it become difficult to track the time history of field variables at a fixed material point;

- cumbersome numerical mapping is required to handle complex geometries and difficulty arises in determining free or moving boundaries and material interfaces

- the computational grid should be large enough to cover also the portion of the space the fluid can move to.

+ large deformation of the continuum do not cause mesh distortion and taint of the numerical solution;

+ no adaptive behavior is needed.

1.3 Meshfree and Meshfree Particle Methods

Even if grid-based numerical methods are consolidated tools for the analysis of advanced problem in both fluid and solid mechanics [**Bontempi et al., 2008**], they suffers from some inherent difficulties which limit their applicability to other fields [**Manenti et al., 2008**].

The basic idea of the meshfree methods is to discretize the continuum through a set of nodes without the connective mesh in order to follow the deformation experienced by the material and avoid the degradation of the numerical result maintaining a suitable computational effort.

When the nodes assumes a physical meaning, i.e. they represent material particles carrying physical properties, the method is said to be meshfree particle and follows, in general, a Lagrangian approach.

Nevertheless there are some examples where particles are fixed in the Eulerian space as interpolation points.

1.4 Advantages of Meshfree Particle Methods

When adopting a discrete set of particles without topological connectivity (i.e. a grid) for representing the material continuum, treatment of large deformation problems is relatively easier.

The particle tracking along with the relevant field variables can be obtained by numerical solution of the discretized set of governing Eq.s.

Representation of free and moving surface becomes an easier task.

There are however some topics related to meshfree particle methods that still requires further study for possible engineering application (e.g. representation of interfaces between different continua, modeling of solid boundaries with complex geometries, fluid and solid dynamic interaction involving structure deformation etc).

1.5 Particle Approximation Principle

The solution strategy of a meshfree particle method is similar as for grid-based method:

domain discretization with a finite number of particles;

numerical discretization of the system of partial differential Eq.s;

numerical technique to solve the resulting ordinary differential Eq.s in transient problems.

In particular the process of numerical discretization involves the approximation of functions, derivatives and integrals at a particle by using the information at all its neighbors, i.e. the surrounding particles that exert an influence on it.

The above procedure is called particle approximation.

2. Basics of the SPH method

2.1 Integral representation and kernel approximation of a function

2.2 Kernel properties and some examples of kernel function

2.3 Kernel approximation of a function derivative

2.4 Particle approximation of a function and its derivative

2.1 Integral Representation of a Function

Smoothed Particle Hydrodynamics was originally developed as a probabilistic meshfree particle method for simulating astrophysical problems [**Lucy, 1977**], [**Gingold & Monaghan, 1977**].

It was later modified as a deterministic meshfree particle method and applied to continuum solid and fluid mechanics [**Monaghan, 1994**], [**Monaghan, 1992**].

The basic step of the method for domain discretization, field function approximation and numerical solution can be summarized as follows [**Liu & Liu, 2007**]:

1. The continuum is decomposed into a set of arbitrarily distributed particles with no connectivity (meshfree);
2. The integral representation method is adopted for field function approximation;
3. Particle approximation is introduced for converting integral representation into finite summation.

2.1 Integral Representation of a Function

The concept of integral representation of a generic function $f(\mathbf{x})$ of the position vector $\mathbf{x}$ used in the SPH method originates from the identity [**Li & Liu, 2004**]:

$$f(\mathbf{x}) = \int_{\Omega} \delta(\mathbf{x} - \mathbf{x}') f(\mathbf{x}') d\Omega_{\mathbf{x}'} \tag{1}$$

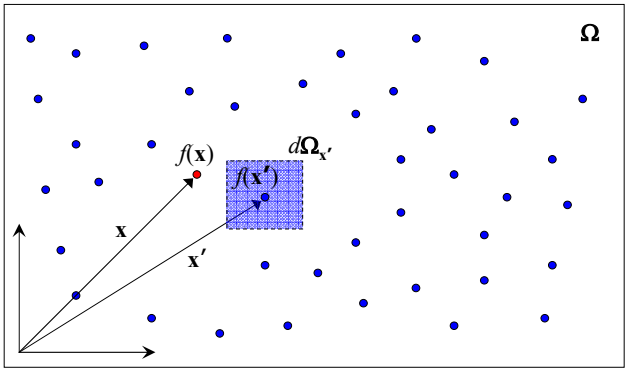

2.1 Integral Representation of a Function

The concept of integral representation of a generic function $f(\mathbf{x})$ of the position vector $\mathbf{x}$ used in the SPH method originates from the identity [**Li & Liu, 2004**]:

$$f(\mathbf{x}) = \int_{\Omega} \delta(\mathbf{x} - \mathbf{x}') f(\mathbf{x}') d\Omega_{\mathbf{x}'} \tag{1}$$

where the function f is defined on the n-dimensional domain Ω, $d\Omega_{x'}$ is the elementary volume surrounding the point at $\mathbf{x}'$ located in the neighborhood of the point at $\mathbf{x}$ and $\delta(\mathbf{x}\text{-}\mathbf{x}')$ is the Dirac delta function defined as (in one-dimensional space):

$$\delta_{\varepsilon}(x - x') = \lim_{\varepsilon \to 0} \begin{cases} 0; & x < x' - \varepsilon/2 \\ 1/\varepsilon; & x' - \varepsilon/2 < x < x' + \varepsilon/2 \\ 0; & x > x' + \varepsilon/2 \end{cases} \tag{2}$$

Since the Dirac delta function lacks some required properties for a "well behaved function" such as continuity and differentiability it is replaced by a kernel function that mimic it.

2.1 Kernel Approximation of a Function

The integral approximation in term of the smoothing interpolant kernel W is thus given by:

$$\langle f(\mathbf{x})\rangle = \int_{\Omega} W(\mathbf{x}-\mathbf{x}',h) f(\mathbf{x}')\, d\Omega_{\mathbf{x}'} \tag{3}$$

In general W is a central function (i.e. it depends on $r=|\mathbf{x}\text{-}\mathbf{x}'|$ which is the modulus of the relative distance) and it is similarly denoted by:

$$\langle f(\mathbf{x})\rangle = \int_{\Omega} W(r,h) f(\mathbf{x}')\, d\Omega_{\mathbf{x}'} \tag{4}$$

The letter h denotes the so called smoothing length.

The kernel function is defined over a compact support $\Omega(\kappa h)$ whose finite extension (κh) is proportional to the smoothing length: W represent an approximation of the Dirac delta function, thus Eq. (4) is said to be the kernel approximation of Eq. (1).

2.2 Properties of Kernel

There are some important features common to the kernel functions usually adopted in fluid and solid dynamic computations:

Normalization condition

$$\int_{\Omega} W(\mathbf{x}-\mathbf{x}',h)\, d\Omega_{\mathbf{x}'} = 1 \tag{5}$$

Delta function property

$$\lim_{h\to 0} W(\mathbf{x}-\mathbf{x}',h) = \delta(\mathbf{x}-\mathbf{x}') \tag{6}$$

Compact support

$$W(\mathbf{x}-\mathbf{x}',h) = 0 \quad \text{if } |\mathbf{x}-\mathbf{x}'| > \kappa h \tag{7}$$

$$\nabla_{\mathbf{x}} W(\mathbf{x}-\mathbf{x}',h) = \frac{\partial W}{\partial r}\frac{(\mathbf{x}-\mathbf{x}')}{|\mathbf{x}-\mathbf{x}'|} = -\nabla_{\mathbf{x}'} W(\mathbf{x}'-\mathbf{x},h) \tag{8}$$

2.2 Examples of Kernel Function

The integral approximation in term of the smoothing interpolant kernel W is thus given by:

Gaussian

$$W(r,h)=\frac{1}{\left(\pi h^2\right)^{n/2}}\exp\left(-r^2/h^2\right) \tag{9}$$

The Gaussian kernel function is adequately smooth even for higher order derivatives and provides stable and accurate results even for disordered particles distributions.

Even if it is not compactly supported it approaches rapidly to zero and can be regarded as compact in numerical computations; however for higher order derivatives the radius of the support may increase significantly in order to assure the above requirement.

2.2 Examples of Kernel Function

The integral approximation in term of the smoothing interpolant kernel W is thus given by:

Cubic spline

$$W(r,h)=\frac{C_n}{h^n}\begin{cases}1-3/2\,\tilde{r}^2+3/4\,\tilde{r}^3; & 0\le\tilde{r}\le 1\\ 1/4\left(2-\tilde{r}\right)^3; & 1\le\tilde{r}\le 2\\ 0; & \text{otherwise}\end{cases} \tag{10}$$

where $\tilde{r}=r/h$ and the normalization factor C_n assumes the following values depending on the problem dimension:

$$C_n=\begin{cases}2/3; & n=1\\ 10/7\pi; & n=2\\ 1/\pi; & n=3\end{cases}$$

This function is widely used due to its narrower support: it resemble a Gaussian function but its second derivatives is piecewise linear function and is thus less smooth and stable when the particle disorder is high.

2.3 Kernel Approximation of a Function derivative

When substituting the generic function f with $\nabla \cdot f$ in Eq. (4) is obtained:

$$\langle \nabla \cdot f(\mathbf{x}) \rangle = \int_{\Omega} [\nabla_{\mathbf{x}'} \cdot f(\mathbf{x}')] W(r,h)\, d\Omega_{\mathbf{x}'} \tag{11}$$

where the derivatives in the nabla operator are taken with respect to the point at $\mathbf{x}'$. By considering the generic identity:

$$[\nabla \cdot f] W = \nabla \cdot [f W] - f \cdot [\nabla W] \tag{12}$$

Substituting into Eq. (11) and applying the divergence theorem it follows:

$$\langle \nabla \cdot f(\mathbf{x}) \rangle = \int_{\partial\Omega} f(\mathbf{x}') W(r,h)\, dS - \int_{\Omega} f(\mathbf{x}') \cdot [\nabla_{\mathbf{x}'} W(r,h)]\, d\Omega_{\mathbf{x}'} \tag{13}$$

2.3 Kernel Approximation of a Function derivative

When substituting the generic functio

$$\langle \nabla \cdot f(\mathbf{x}) \rangle = \int_{\Omega} [\nabla$$

where the derivatives in the nabla op
considering the generic identity:

$$[\nabla \cdot f] W = \nabla$$

Substituting into Eq. (11) and applyin

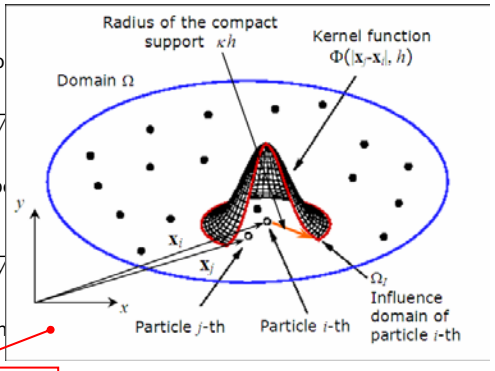

$$\langle \nabla \cdot f(\mathbf{x}) \rangle = \int_{\partial\Omega} f(\mathbf{x}') W(r,h)\, dS - \int_{\Omega} f(\mathbf{x}') \cdot [\nabla_{\mathbf{x}'} W(r,h)]\, d\Omega_{\mathbf{x}'} \tag{13}$$

The first integral on the right-hand side is evaluated on the surface elements dS of the frontier $\partial\Omega$ of the integration domain Ω: if the compact support of W falls within Ω the surface, this integral must be zero according to Eq. (7).

2.3 Kernel Approximation of a Function derivative

In virtue of the kernel property defined by Eq. (8) it results:

$$\langle \nabla \cdot f(\mathbf{x}) \rangle = \int_{\Omega(\kappa h)} f(\mathbf{x}') \cdot [\nabla_{\mathbf{x}} W(r,h)] \, d\Omega_{\mathbf{x}'} \tag{14}$$

or simply:

$$\langle \nabla \cdot f(\mathbf{x}) \rangle = \int_{\Omega(\kappa h)} f(\mathbf{x}') \cdot [\nabla W(r,h)] \, d\Omega_{\mathbf{x}'} \tag{14'}$$

Eq. (14′) means that the differential operation on the function f is shifted on the smoothing function W.

2.4 Particle Approximation

At the generic i-th point the discrete form of the integral kernel approximation for the set of material particles representing the discretized continuum can be obtained by the so called particle approximation (denoted by $\langle f(\mathbf{x}_i) \rangle$):

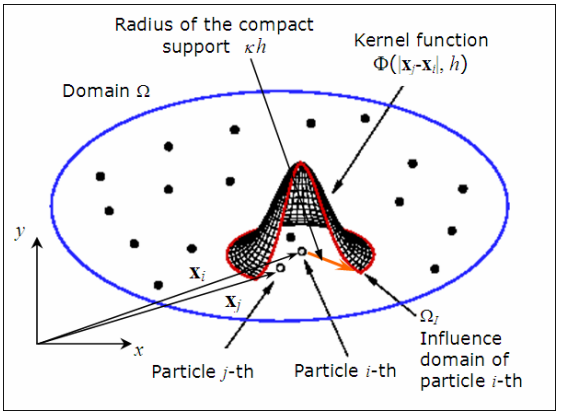

$$\langle f(\mathbf{x}_i) \rangle = \int_{\Omega_I} W(r_{ij}, h) f(\mathbf{x}_j) \, d\Omega_{\mathbf{x}_j}$$

$$\cong \sum_{j=1}^{N} f(\mathbf{x}_j) W(r_{ij}, h) \frac{m_j}{\rho_j}$$

The summation is extended to the N neighboring particles with volume $\Delta V_j = m_j / \rho_j$ in the compact support (or influence domain) Ω_I of the i-th particle.

The symbol $r_{ij} = |\mathbf{x}_i - \mathbf{x}_j|$ denotes the modulus of the relative distance.

2.4 Particle Approximation

At the generic i-th point the discrete form of the integral kernel approximation for the set of material particles representing the discretized continuum can be obtained by the so called particle approximation (denoted by $\langle f(\mathbf{x}_i)\rangle$):

$$\begin{aligned}\langle f(\mathbf{x}_i)\rangle &= \int_{\Omega_I} W(r_{ij},h) f(\mathbf{x}_j)\, d\Omega_{\mathbf{x}_j} \\ &\cong \sum_{j=1}^{N} f(\mathbf{x}_j) W(r_{ij},h) \frac{m_j}{\rho_j}\end{aligned} \qquad (15)$$

The estimate of the function f is thus carried out as the sum of the values it assumes on the neighboring points within the support weighted by the smoothing function W.

2.4 Particle Approximation

Thus for the generic i-th particle the discrete particle approximation yields the following estimate of the function and its derivative based on the information contained at the neighboring particles in the support domain Ω_I:

$$\begin{aligned}\langle f(\mathbf{x}_i)\rangle &= \sum_{j=1}^{N} \frac{m_j}{\rho_j} f(\mathbf{x}_j) W(r_{ij},h) \\ \langle \nabla \cdot f(\mathbf{x}_i)\rangle &= \sum_{j=1}^{N} \frac{m_j}{\rho_j} f(\mathbf{x}_j) \cdot \nabla W(r_{ij},h)\end{aligned} \qquad (16)$$

From the above Eq.s it results that particle approximation allows to estimate the field variables without using a topological connective grid between the particles for carrying out the numerical integration.

2.4 Particle Approximation Properties

It is worth to note that the following properties exists for the particle approximation:

$$\begin{aligned}\langle f_1 + f_2 \rangle &= \langle f_1 \rangle + \langle f_2 \rangle \\ \langle c\, f_1 \rangle &= c \langle f_1 \rangle \\ \langle f_1 f_2 \rangle &= \langle f_1 \rangle \langle f_2 \rangle\end{aligned} \tag{17}$$

where c is a constant. The first and second relation states that the estimate <> is a linear operator.

2.4 Particle Approximation

Alternative expressions for the derivative of the generic function f could be obtained by considering the following identities:

$$\rho \nabla \cdot f = \nabla \cdot (\rho f) - f \cdot \nabla \rho \tag{18}$$

$$\frac{\nabla \cdot f}{\rho} = \frac{f}{\rho^q} \cdot \nabla \left(\frac{1}{\rho^{1-q}} \right) + \frac{1}{\rho^{2-q}} \nabla \cdot \left(\frac{f}{\rho^{q-1}} \right) \tag{19}$$

being q an integer.

Since the particle approximation is a linear operator, by substituting Eq. (18) or (19) into the latter of Eq. (16) it follows respectively:

$$\rho_i \langle \nabla \cdot f(\mathbf{x}_i) \rangle = \sum_{j=1}^{N} m_j \left[f(\mathbf{x}_j) - f(\mathbf{x}_i) \right] \cdot \nabla W(r_{ij}, h) \tag{20}$$

$$\frac{1}{\rho_i} \langle \nabla \cdot f(\mathbf{x}_i) \rangle = \sum_{j=1}^{N} m_j \left[\frac{f(\mathbf{x}_j)}{\rho_j^q} \frac{1}{\rho_i^{2-q}} + \frac{f(\mathbf{x}_i)}{\rho_i^q} \frac{1}{\rho_j^{2-q}} \right] \cdot \nabla W(r_{ij}, h) \tag{21}$$

3. Implementation of Navier-Stokes Eq.s

3.1 Derivation of governing Eq.s (Navier-Stokes Eq.s)

3.2 SPH formulation of Navier-Stokes Eq.s

3.3 Other numerical aspects relevant to SPH

3.4 Boundary conditions

3.1 Mass Balance or Continuity Eq.

According classical mechanics the mass of a fluid system is unchanged regardless of its state of motion.

When considering a fluid element, the mass balance Eq. states that the time rate of change of the specific mass within the volume must equates the net flow in each coordinate direction; it can thus be obtained (summation over repeated indices is assumed):

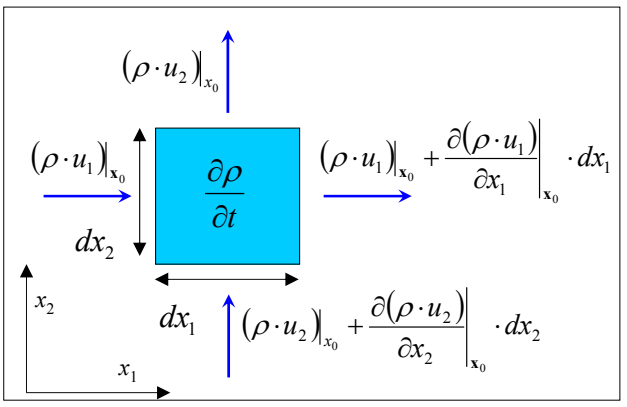

$$\frac{\partial \rho}{\partial t} + \frac{\partial (\rho \cdot u_j)}{\partial x_j} = 0 \qquad (22)$$

3.1 Mass Balance or Continuity Eq.

By solving the product in the partial derivative of the second term on the left-hand side of Eq. (22) and applying the Reynolds Transport Theorem follows:

$$\frac{D\rho}{Dt}+\rho\frac{\partial u_j}{\partial x_j}=0 \quad \text{or} \quad \frac{D\rho}{Dt}+\rho\nabla\cdot\mathbf{u}=0$$

$$\text{with} \quad \frac{D\rho}{Dt}=\frac{\partial\rho}{\partial t}+u_j\frac{\partial\rho}{\partial x_j} \tag{23}$$

When considering an incompressible flow the time rate of change of mass when following a material fluid particle should be zero (i.e. $D\rho/Dt=0$):

$$\frac{\partial u_j}{\partial x_j}=0 \quad \text{or} \quad \nabla\cdot\mathbf{u}=0 \tag{24}$$

3.1 Momentum Balance Eq.

When applying the Newton Second Law to the material fluid particle of volume δV, the net force $\mathbf{F}$ it experiences must equals the product of its mass times the acceleration:

$$\frac{D(\rho\,\delta V\,u_i)}{Dt}=F_i \quad i=1,2,3 \tag{25}$$

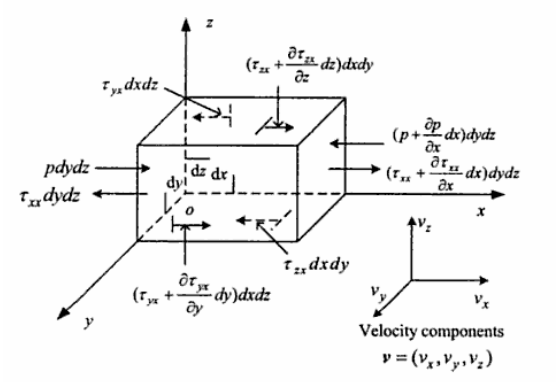

The net force $\mathbf{F}=(F_1,F_2,F_3)$ is made up, for a fluid particle, of three contributions: body force, pressure force, viscous force.

3.1 Momentum Balance Eq.

When applying the Newton Second Law to the material fluid particle of volume δV, the net force $\mathbf{F}$ it experiences must equals the product of its mass times the acceleration:

$$\frac{D(\rho \delta V u_i)}{Dt} = F_i \quad i = 1,2,3 \tag{25}$$

By assuming body term due to the gravity only and that the axis x_3 is directed upward, Eq. (26) turns into (summation over repeated indices is assumed):

$$\underbrace{\frac{\partial u_i}{\partial t}}_{\text{Local term}} + \underbrace{u_j \frac{\partial u_i}{\partial x_j}}_{\text{Convective term}} = -\frac{1}{\rho}\frac{\partial (p + \rho g x_3)}{\partial x_i} + \frac{1}{\rho}\frac{\partial \tau_{ij}}{\partial x_j} \quad i = 1,2,3 \tag{27}$$

The left-hand side term of Eq. (27) (i.e. the material or Lagrangian derivative) has been rewritten in Eulerian form through the Reynolds Transport Theorem: the time rate of change following the particle motion D/Dt consists of a local time rate of change (non-stationary field) and a convective term related to particle velocity (convective transport).

3.1 Momentum Balance Eq.

When considering a Newtonian fluid the viscous stress tensor τ_{ij} is proportional to the strain rate tensor ε_{ij} through a constant coefficient called dynamic viscosity μ:

$$\tau_{ij} = \mu \varepsilon_{ij} = \mu \left[\frac{\partial u_i}{\partial x_j} + \frac{\partial u_j}{\partial x_i} - \frac{2}{3}\frac{\partial u_k}{\partial x_k}\delta_{ij} \right] \tag{28}$$

where δ_{ij} is the Kronecker delta. Substituting into Eq. (27) yields:

$$\frac{\partial u_i}{\partial t} + u_j \frac{\partial u_i}{\partial x_j} = -\frac{1}{\rho}\frac{\partial (p + \rho g x_3)}{\partial x_i} + \frac{\mu}{\rho}\left[\frac{\partial^2 u_i}{\partial x_j^2} + \frac{1}{3}\frac{\partial}{\partial x_i}\frac{\partial u_j}{\partial x_j} \right] \quad i = 1,2,3 \tag{29}$$

$$\text{or} \quad \frac{D\mathbf{u}}{Dt} = -\frac{1}{\rho}\nabla(p + \rho g x_3) + \frac{\mu}{\rho}\left[\nabla \cdot \nabla \mathbf{u} + \frac{1}{3}\nabla(\nabla \cdot \mathbf{u}) \right]$$

where the ratio μ/ρ is the dynamic viscosity often denoted by ν.

3.2 SPH Formulation of Governing Eq.s

The SPH formulation of the Continuity Eq. can be obtained through the particle approximation procedure by taking into account the properties in Eq.s (17).

By considering the identity (20)

$$\rho_i \langle \nabla \cdot f(\mathbf{x}_i) \rangle = \sum_{j=1}^{N} m_j \left[f(\mathbf{x}_j) - f(\mathbf{x}_i) \right] \cdot \nabla W(r_{ij}, h) \tag{20}$$

the continuity Eq. (23)

$$\frac{D\rho}{Dt} = -\rho \nabla \cdot \mathbf{u} \tag{23}$$

with the assumption of the identity $W(r_{ij},h)=W_{ij}$ becomes in the particle approximation:

$$\left\langle \frac{D\rho}{Dt} \right\rangle_i = -\sum_{j=1}^{N} m_j (\mathbf{u}_j - \mathbf{u}_i) \cdot \nabla W_{ij} \tag{31}$$

3.2 SPH Formulation of Governing Eq.s

The SPH formulation of the Momentum Eq.s can be obtained through the particle approximation procedure by taking into account the properties in Eq.s (17).

From the Eq. (21) with q=2:

$$\frac{1}{\rho_i} \langle \nabla \cdot f(\mathbf{x}_i) \rangle = \sum_{j=1}^{N} m_j \left[\frac{f(\mathbf{x}_j)}{\rho_j^2} + \frac{f(\mathbf{x}_i)}{\rho_i^2} \right] \cdot \nabla W(r_{ij}, h) \tag{21'}$$

and from the latter of Eq.s (29)

$$\frac{D\mathbf{u}}{Dt} = -\frac{1}{\rho} \nabla (p + \rho g x_3) + \frac{\mu}{\rho} \left[\nabla \cdot \nabla \mathbf{u} + \frac{1}{3} \nabla (\nabla \cdot \mathbf{u}) \right] \tag{29}$$

considering an inviscid fluid (i.e. μ=0) follows:

$$\left\langle \frac{D\mathbf{u}}{Dt} \right\rangle_i = -\sum_{j=1}^{N} m_j \left(\frac{p_i}{\rho_i^2} + \frac{p_j}{\rho_j^2} \right) \cdot \nabla W_{ij} + \mathbf{g} \tag{32}$$

being $\mathbf{g}$ the gravity acceleration vector.

3.2 SPH Formulation of Governing Eq.s

In the Eq. (32) usually an additional term is added to the pressure term for achieving numeric stability especially when simulating shock wave front. Based on the von Neumann-Richtmyer artificial viscosity for converting kinetic energy into heat during sudden compression of the continuum, **Monaghan (1989)** propose the following formulation which also prevents particles penetration:

$$\Pi_{ij} = \begin{cases} \dfrac{-\alpha_M \, 0.5\left(c_{s\,i} + c_{s\,j}\right)\phi_{ij} + \beta_M \, \phi_{ij}^2}{0.5\left(\rho_i + \rho_j\right)} & \text{if} \quad \mathbf{u}_{ij} \cdot \mathbf{x}_{ij} < 0 \\ 0 & \text{if} \quad \mathbf{u}_{ij} \cdot \mathbf{x}_{ij} > 0 \end{cases} \tag{33}$$

where $c_{s\,i}$ and $c_{s\,j}$ are the sound speed of particle i and particle j respectively, α_M and β_M are non-dimensional coefficients (typically β_M=0) and ϕ_{ij}:

$$\mu_{ij} = \frac{h\,\mathbf{u}_{ij} \cdot \mathbf{x}_{ij}}{x_{ij}^2 + (0.1h)^2} \tag{33'}$$

3.2 SPH Formulation of Governing Eq.s

The hypothesis of weakly compressible fluid is assumed: this is valid as long as the local deviations of the fluid density from the reference value ρ_0 remain sufficiently small.

Such an hypothesis allows to adopt a relatively large time increment (which must satisfies the Courant condition) thus producing positive effects concerning the required computational resources.

For a single phase physical system the adopted form of the state equation is:

$$\frac{p}{p_0} = K\left(\frac{\rho}{\rho_0}\right)^{\gamma} - 1 \tag{34}$$

with p_0 the reference pressure, K and γ coefficients related to fluid properties and thermodynamic status. Eq. (34) allows to decuple the dynamic and cinematic problem.

The hypothesis of weakly compressible fluid implies that the Mach number remains sufficiently small; according to **Monaghan (1994)** the following condition have to be satisfied, with u a characteristic velocity of the problem:

$$\mathrm{Ma} = \frac{u}{c_s} \cong 0.1 \tag{35}$$

3.3 Other Numerical Aspects

XSPH: this variant, proposed by **Monaghan (1994)**, corrects particle velocity assuring more ordered flow and prevents penetration between continua when high speed or impact occur.

$$\mathbf{u}_i^{XSPH} = \mathbf{u}_i + \varepsilon \sum_{j=1}^{NP} \frac{m_j (\mathbf{u}_j - \mathbf{u}_i)}{0.5(\rho_i + \rho_j)} W_{ij} \qquad (36)$$

Tensile instability: causes exponential growth of particles velocity for small perturbation of their position in a region of the continuum with a tensile state of stress. When compression occurs clumping of particles may took place. Modified kernel function have been proposed for remedial [**Morris, 1996**].

Correction of kernel: particles near free surface are characterized by a truncated kernel function due to the lack of neighbors. The normalization condition in Eq. (5) is no more satisfied and a possible solution is to multiply the kernel function for a normalization factor such as:

$$W_{ij}^{\text{norm}} = \frac{W_{ij}}{\left(\sum_{j=1}^{N} W_{ij} \frac{m_j}{\rho_j} \right)} \qquad (37)$$

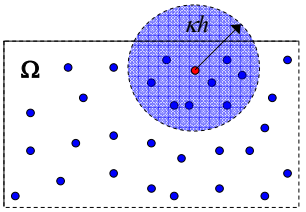

3.3 Normalization of Kernel Derivatives

The effect induced by non-uniform covering of the support domain due to particle disorder lead to an inaccurate estimate of the derivatives of the trial function $f = 1 + 4x^2 + 4y^2$ [**Falappi, 2006**].

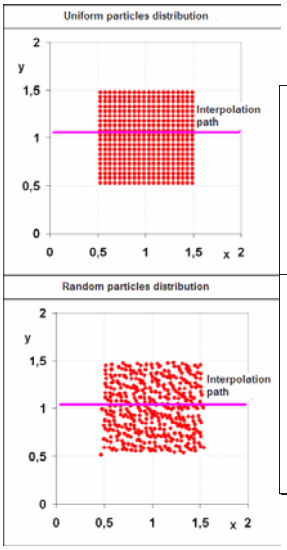

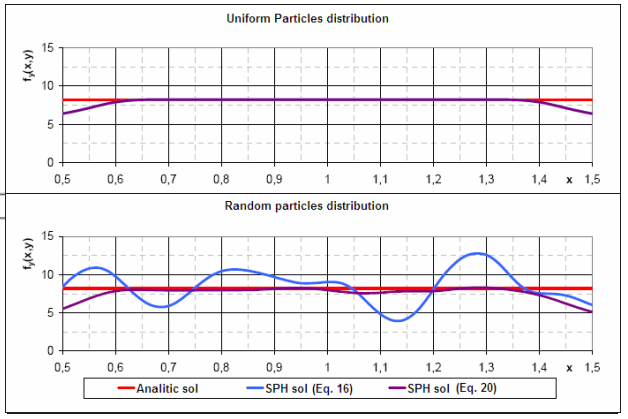

3.3 Normalization of Kernel Derivatives

A normalization technique based on the Taylor series expansion of the kernel function can be adopted for enhancing the solution accuracy of the SPH interpolation even near the free-boundaries.

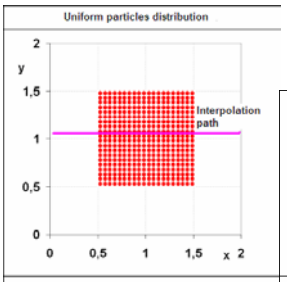

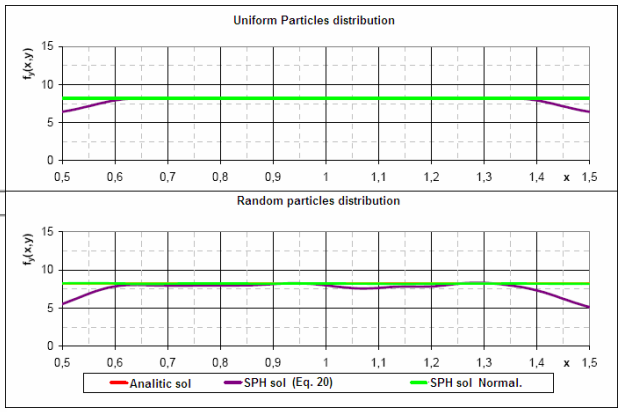

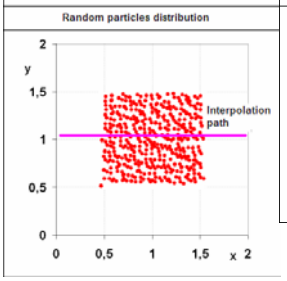

3.3 Other Numerical Aspects

Neighboring particles searching: particle approximation need to know the neighbors of a particle Pi to estimate the field variable at that point; neighbors of Pi are those particles inside the influence domain of Pi. Since computational point are not connected each other, neighbors of the generic particle changes in time as the fluid evolves in space and should be searched continuously.

Even if different approaches exists for neighboring particle searching [**Liu & Liu, 2007**], linked list algorithm is widely adopted for constant smoothing length.

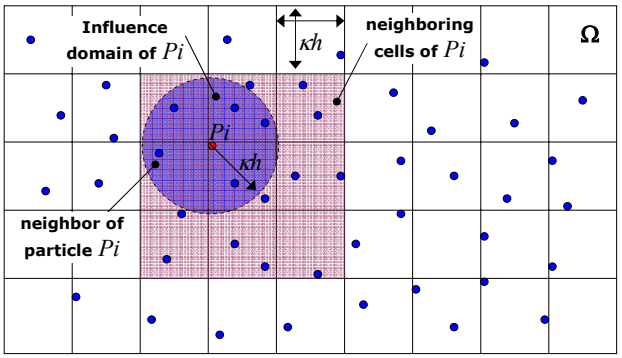

A mesh is overlaid on the computational domain and all particles are assigned to the corresponding cell through a linked list: the search of the neighbors of Pi restricts to the particles in the surrounding cell of Pi.

3.3 Solution Strategy

The following procedure provides a typical solution strategy for solving the governing Eq.s in the SPH method:

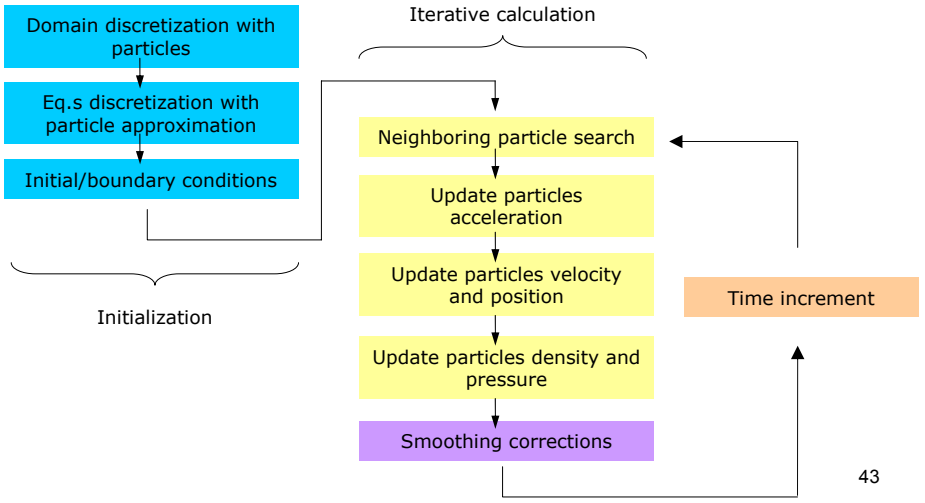

3.4 Boundary Conditions (Boundary Forces)

In astrophysical problem no solid boundary exists; with the extension of the SPH method to fluid mechanic computations several approaches for treating boundary conditions were developed:

Monaghan & Koss (1999) proposed a technique based on the Lennard-Jones formulation for the intermolecular repulsive force. This method, so called boundary forces method, is based on the distribution of fixed "guard" particles along the boundaries which exerts suitable forces on the nature of the problem as function of the distance between the boundary and the inner particle.

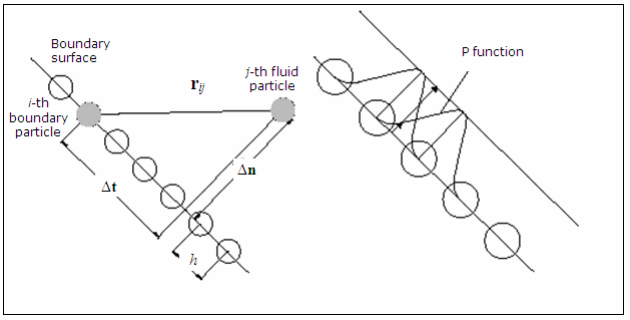

3.4 Boundary Conditions (Ghost Particles)

A different methodology for simulating solid boundary [**Libersky et al., 1993**] is to create, at each time step, additional particles as reflected images of the fluid particles located within a layer near the boundaries (seen as mirrors); the density (pressure) and velocity of each of these ghost particles are assigned so as to accomplish conditions of reflection or linear extension.

This method appears to be the most rigorous even if it become very cumbersome for three-dimensional complex geometries.

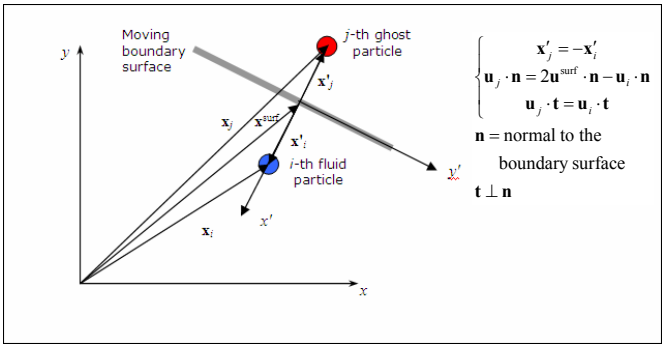

3.4 Boundary Conditions (Semi-Analytic Integral)

This method is based on a direct evaluation of the boundary contributions to the SPH approximation of the fluid-dynamic equations through the analytical computation of integral terms [**Di Monaco et al., 2009**].

The solid boundary is replaced by the fluid which extends out with a suitable distribution of velocity and pressure: unlike ghost particle method, the boundary is supposed to be continuous (i.e. made up of infinite particles).

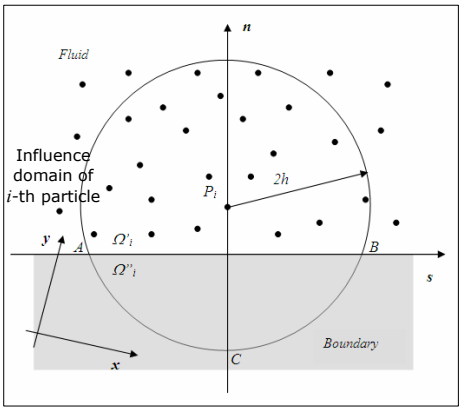

4. Numerical Applications of the SPH method

4.1 One-dimensional wave generation

4.2 Coupled moving boundary

4.3 Sediment flushing

4.4 Three-dimensional dambreak

4.1 One-Dimensional Wave Generation

A flume with piston-type wavemaker has been simulated for generating regular wave trains.

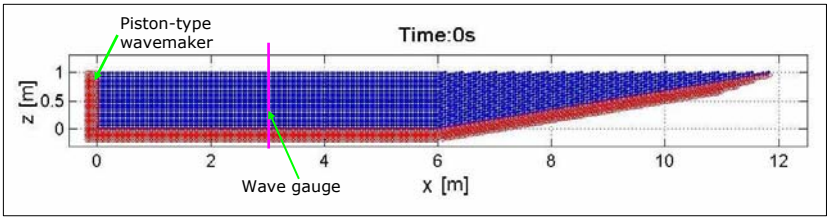

The analytical solution [**Biésel, 1951**] provides the reference for evaluating the numerical results at the wave gauge.

Transfer function

$$\frac{H}{S_0} = \frac{4\sinh^2(k\,h)}{\sinh(2kh)+2kh}$$

Surface elevation (far field)

$$\eta(x,t) = a_0 \cosh(k\,h)\cos(\omega t - kx)$$

$$a_0 = \frac{2\omega^2}{g\,k}\,\frac{S_0 \sinh(k\,h)}{\sinh(2kh)+2kh}$$

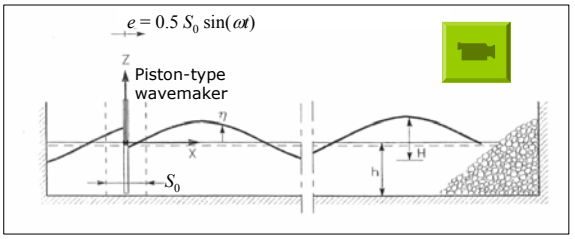

4.2 Coupled Moving Boundary

A floating box with one degree of freedom (heave) is simulated in the wave flume.

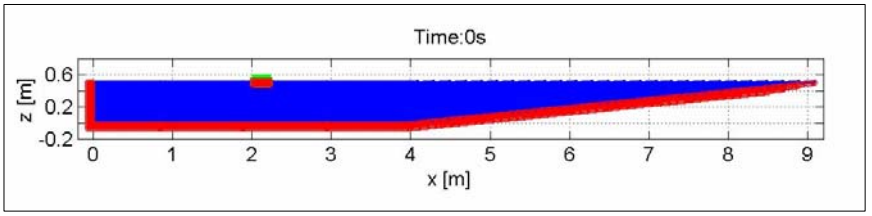

Numerical results are compared with experimental data [**Manenti et al., 2008**].

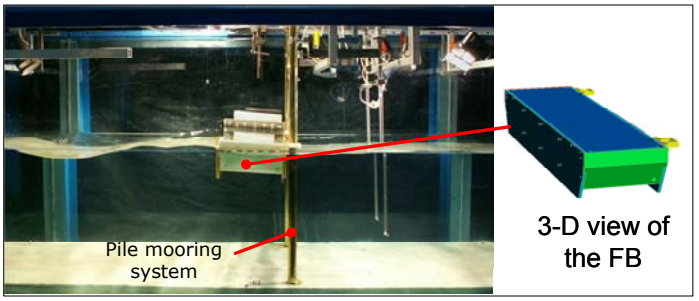

4.3 Sediment Flushing

Physical and numerical two-dimensional model of sediment flushing during the opening of a bottom outlet of a dam [**Agate et al., 2009**], [**Manenti et al, 2009**].

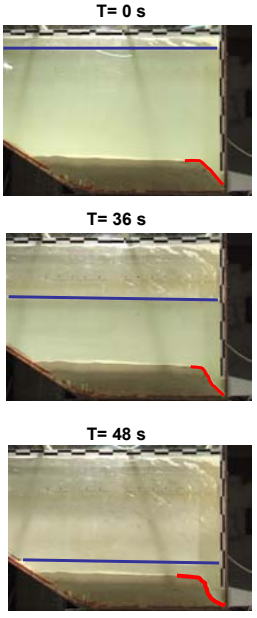

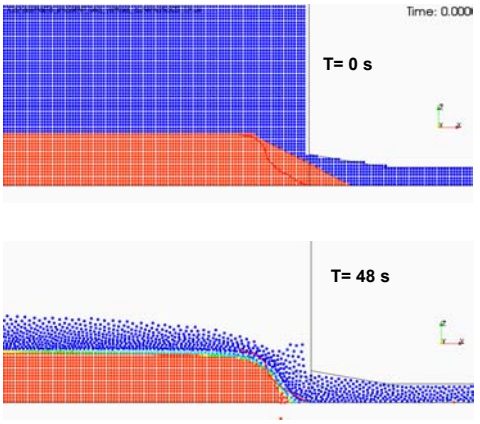

4.4 Three-Dimensional Dambreak

A general approach for modeling solid boundaries with the integral semi-analytic technique has been developed for handling complex three-dimensional geometries [**Di Monaco et al., 2009**].

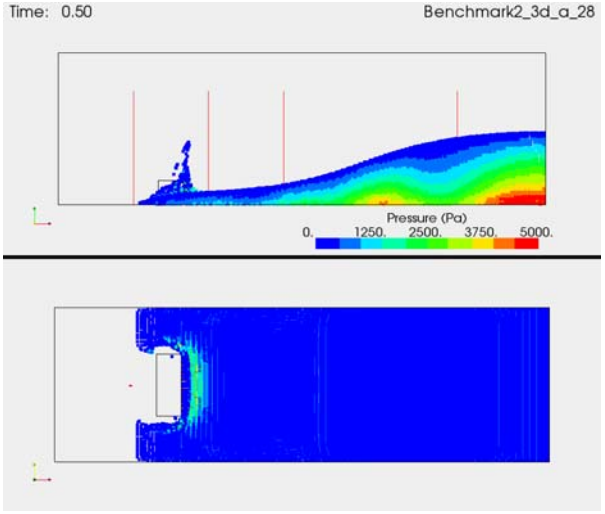

Bibliographic References

Agate G., Guandalini R. 2009 "Strumenti numerici a scala di dettaglio per problemi idrodinamici in impianti idroelettrici". Pub. 08006002.

Bontempi F., Li H., Petrini F., Manenti S. 2008 "Numerical modeling for the analysis and design of offshore wind turbines", ASEM'08 Int. Conf. (Korea).

Di Monaco A., Manenti S., Agate G., Gallati M., Guandalini R., Maffio A., Sibilla S. 2009 "A semi-analytic approach for SPH modeling of solid boundaries". Proc. 4th SPHERIC Int. Workshop (France), pp. 165-171.

Falappi S. 2006 "Simulazioni numeriche di flussi di fluidi viscosi e materiali granulari con la tecnica SPH", PhD dissertation, Università degli Studi di Pavia (in Italian).

Gingold R.A., Monaghan J.J. 1977 "Smoothed particle hydrodynamics: theory and application to non-spherical stars", Mon Not Roy Astron Soc, 181-375.

Li S., Liu W.K. 2004 "Meshfree Particle Methods", Springer Ed.

Libersky L.D., Petschek A.G., CarneyT.C., Hipp J.R., Allahady F.A. 1993 "High strain Lagrangian hydrodynamics", J. Comp. Physics 109, 67.

Lin P. 2008 "Numerical modeling of water waves", Taylor & Francis Ed.

Liu G.R., Liu M.B. 2007 "Smoothed Particle Hydrodynamics - a Meshfree Particle Methods", World Scientific Publ.

Lucy L. 1977 "A numerical approach to the fission hypothesis", Astron J., 82-1013.

Manenti S., Di Monaco A., Agate G., Gallati M., Guandalini R., Maffio A., Sibilla S. 2009 "Simulating rapid sediment scour by water flow with SPH", Proc. 4th SPHERIC Int. Workshop (France), pp. 144-148.

Bibliographic References

Manenti S., Ruol P. 2008 "Fluid-Structure Interaction in Design of Offshore Wind Turbines: SPH Modeling of Basic Aspects", Proc. Int. Workshop Handling Exception in Structural Engineering (Italy) DOI: 10.3267/HE2008.

Manenti S., Ravaglioli U. 2006a "Thermal stresses evaluation and safety aspects associated with massive concrete constructions joined to existing structures: the case of a masonry gravity dam". Proc. 8th Int. Conf. on Comp. Struct. Tech. (Spain) DOI: 10.4203/ccp.83.83.

Manenti S., Cecconi G. 2006b "Evaluation of wave damages in urbanized lagoons". Proc. 8th Int. Conf. on Comp. Struct. Tech. (Spain) DOI: 10.4203/ccp.83.185.

Monaghan J.J., Kos A. 2000 "Scott Russell's wave generator", Physics of Fluids 12, 622-630.

Monaghan J.J. 1994 "Simulating free surface flows with SPH", J. Comput. Phys. Vol. 110, 399-406.

Monaghan J.J. 1992 "Smoothed particle hydrodynamics", Ann. Rev. Astronomy and Astrophysics, Vol. 30, 543-574.

Monaghan J.J. 1989 "On the problem of penetration in particle methods", J. Comp. Phys., Vol. 82: 1-15.

Morris J.P. 1996 "Stability properties of SPH". Publ. Astrn. Soc. Aust. Vol.13, pp. 97-112.

Prager W. 1961 "Introduction to mechanics of continua", Ginn and Company

Zienkiewicz O.C., Taylor R.L. 1989 "The Finite Element Method", Vol. I 4th ed. McGraw-Hill.